Atmos. Chem. Phys., 12, 3393–3404, 2012
www.atmos-chem-phys.net/12/3393/2012/
doi:10.5194/acp-12-3393-2012

Atmospheric Chemistry and Physics

Influence of aerosols and thin cirrus clouds on the GOSAT-observed CO_2: a case study over Tsukuba

O. Uchino[1], N. Kikuchi[1], T. Sakai[2], I. Morino[1], Y. Yoshida[1], T. Nagai[2], A. Shimizu[1], T. Shibata[3], A. Yamazaki[2], A. Uchiyama[2], N. Kikuchi[1], S. Oshchepkov[1], A. Bril[1], and T. Yokota[1]

[1]National Institute for Environmental Studies, 16-2 Onogawa, Tsukuba, Ibaraki 305-8506, Japan
[2]Meteorological Research Institute, 1-1 Nagamine, Tsukuba, Ibaraki 305-0052, Japan
[3]Graduate School of Environmental Studies, Nagoya University, D2-1(510) Furo-cho, Chikusa-ku, Nagoya 464-8601, Japan

Correspondence to: O. Uchino (uchino.osamu@nies.go.jp)

Received: 12 October 2011 – Published in Atmos. Chem. Phys. Discuss.: 8 November 2011
Revised: 24 February 2012 – Accepted: 19 March 2012 – Published: 10 April 2012

Abstract. Lidar observations of vertical profiles of aerosols and thin cirrus clouds were made at Tsukuba (36.05° N, 140.12° E), Japan, to investigate the influence of aerosols and thin cirrus clouds on the column-averaged dry-air mole fraction of carbon dioxide (XCO_2) retrieved from observation data of the Thermal And Near-infrared Sensor for carbon Observation Fourier Transform Spectrometer, measured in the Short-Wavelength InfraRed band (TANSO-FTS SWIR), onboard the Greenhouse gases Observing SATellite (GOSAT). The lidar system measured the backscattering ratio, depolarization ratio, and/or the wavelength exponent of atmospheric particles. The lidar observations and ground-based high-resolution FTS measurements at the Tsukuba Total Carbon Column Observing Network (Tsukuba TCCON) site were recorded simultaneously during passages of GOSAT over Tsukuba.

GOSAT SWIR XCO_2 data (Version 01.xx) released in August 2010 were compared with the lidar and Tsukuba TCCON data. High-altitude aerosols and thin cirrus clouds had a large impact on the GOSAT SWIR XCO_2 results. By taking into account the observed aerosol/cirrus vertical profiles and using a more adequate solar irradiance database in the GOSAT SWIR retrieval, the difference between the GOSAT SWIR XCO_2 data and the Tsukuba TCCON data was reduced. The 3-band retrieval approach where the aerosol and cirrus profiles were retrieved gave us the best results and the retrieved XCO_2 data followed the seasonal cycle of ∼8 ppm observed at Tsukuba TCCON site.

1 Introduction

The concentration of carbon dioxide (CO_2) increased from about 280 ppm in pre-industrial times (before 1750) to 386.8 ppm in 2009, primarily because of emissions from combustion of fossil fuels and land-use changes (IPCC, 2007; WMO, 2010). Because CO_2 absorbs infrared radiation from the earth's surface, increased CO_2 concentrations lead to a rise in the earth's surface temperature. These changes in temperature influence the biosphere, and the biosphere changes can have a feedback effect on CO_2 concentrations (Cox et al., 2000). To accurately predict future atmospheric CO_2 concentrations and their impacts on climate, it is necessary to accurately quantify the global distribution and variations of CO_2 sources and sinks.

Current CO_2 flux estimates obtained by inverse modeling rely mainly on ground-based observation data. Errors in the estimated regional fluxes in Siberia, Africa, Australia, and South America are particularly large because ground-based monitoring stations are sparse in those regions (WMO, 2010). Spectroscopic remote sensing from space is capable of acquiring data that cover the globe and if those data are accurate and precise enough, it is expected to reduce errors in the CO_2 flux estimation obtained by using inverse modeling (Rayner and O'Brien, 2001; Chevallier et al., 2009; Hungershoefer et al., 2010).

To improve regional CO_2 flux estimates, the Greenhouse gases Observing SATellite (GOSAT) was launched on 23 January 2009 (Kuze et al., 2009) to observe global distributions of CO_2 and methane (CH_4) concentrations from space. Column-averaged dry-air mole fractions of CO_2 and CH_4

(XCO_2 and XCH_4) are retrieved from the Short-Wavelength InfraRed (SWIR) observation data of the Thermal And Near-infrared Sensor for carbon Observation Fourier Transform Spectrometer (TANSO-FTS) onboard GOSAT (Yoshida et al., 2011). Morino et al. (2011) preliminarily validated the GOSAT SWIR XCO_2 and XCH_4 results by comparing them with reference data obtained by a ground-based high-resolution FTS of the Total Carbon Column Observing Network (TCCON; Wunch et al., 2011a). They found that the GOSAT SWIR XCO_2 and XCH_4 (Ver. 01.xx) values were systematically underestimated by 8.85 ± 4.75 ppm and 20.4 ± 18.9 ppb, respectively. To improve the accuracy of the retrieval results, the causes of these biases (systematic errors) need to be investigated.

Houweling et al. (2005) demonstrated that systematic errors in CO_2 satellite remote sensing data can be caused by aerosols by performing model calculations that showed large sensitivity of the CO_2 column to the vertical aerosol profile. To minimize the errors due to aerosols in SWIR CO_2 measurements from space, Butz et al. (2009) proposed that the amount, vertical distribution, and microphysical properties of aerosol particles should be parameterized and retrieved simultaneously with the total CO_2 column. Also, some sensitivity studies of aerosols and/or thin cirrus clouds on XCO_2 measured from space have been made (Kuang et al., 2002; Connor et al., 2008; Reuter et al., 2010; Boesch et al., 2011).

The GOSAT SWIR retrieval algorithm in Ver. 01.xx assumes that aerosols are uniformly distributed below 2 km of altitude and that no cirrus clouds are present. These assumptions are too simple; therefore, a forward spectrum error due to these assumptions may be one of the major sources of error in GOSAT SWIR XCO_2 and XCH_4 data. In this study, we investigated the impact of vertical aerosol profiles and thin cirrus clouds observed by lidar and sky radiometer on the GOSAT SWIR retrieval results, focusing on the GOSAT SWIR XCO_2 results. First, we compare the GOSAT SWIR XCO_2 data with reference data obtained by a ground-based high-resolution FTS at the National Institute for Environmental Studies (NIES) in Tsukuba, which is part of TCCON (hereafter Tsukuba TCCON FTS). Next, we show that GOSAT SWIR XCO_2 data are greatly influenced by high-altitude aerosols and thin cirrus clouds observed by lidar. Finally, we demonstrate that by taking into account the vertical aerosol profiles and thin cirrus clouds observed by lidar and sky radiometer, and by using Toon's solar irradiance database (G. C. Toon, personal communication, 2011; Toon et al., 1999) instead of Kurucz's database, the difference between the GOSAT SWIR XCO_2 data and the Tsukuba TCCON data becomes much less.

2 Comparison of GOSAT SWIR and Tsukuba TCCON XCO_2 data

2.1 GOSAT SWIR XCO_2

We used GOSAT SWIR XCO_2 Ver. 01.xx products. The Ver. 01.xx retrieval algorithm uses TANSO-FTS Band 1 (12 900–13 200 cm^{-1}) and Band 2 (5800–6400 cm^{-1}) to simultaneously derive XCO_2 and XCH_4. To reduce biases, auxiliary parameters such as surface pressure and aerosol optical thickness (AOT) are retrieved together with XCO_2 and XCH_4. The GOSAT SWIR Ver. 01.xx algorithm focuses on those data obtained under cloud-free conditions, and cloud-contaminated data detected by the TANSO Cloud and Aerosol Imager (TANSO-CAI) onboard GOSAT and TANSO-FTS Band 3 (4800–5200 cm^{-1}) data are excluded from the retrieval analysis. After the retrieval calculations, the quality of the retrieved state is checked from the viewpoints of the convergence (number of iterations, chi-squared, and mean square of the residual spectra for each retrieval sub-band), available information (degrees of freedom for signals and the signal-to-noise ratio, SNR), and the range of the retrieved AOT values. Details are described by Yoshida et al. (2011).

2.2 Tsukuba TCCON FTS

Solar absorption spectra are measured with a Bruker IFS 120 HR FTS at NIES (36.05° N, 140.12° E, 31 m a.s.l.) in Tsukuba, Japan. Direct solar light is introduced into the FTS with a solar tracker and five gold-coated flat mirrors. The solar tracker is mounted inside a dome on the roof of the building where the FTS is housed. Measurements with the high-resolution FTS are performed according to the TCCON data protocol. A CaF_2 beam splitter and an InGaAs detector are used for the 5500–10 500 cm^{-1} spectral region. A spectral resolution of 0.02 cm^{-1} (defined as 0.9/maximum optical path difference), an aperture size of 0.5 mm, and a scanner velocity of 10 kHz are used as standard parameters for the TCCON measurements. The pressure in the FTS is kept at ~0.03 Torr by an oil-free scroll vacuum pump. The forward and backward scanned interferograms are separately integrated over a period of about 70 s. A weather station also observes meteorological data, recording surface pressure, surface temperature, relative humidity, wind direction and speed, rainfall, and solar radiation intensity at the same site. Table 1 lists the characteristics of the Tsukuba TCCON FTS. Each measured spectrum was obtained by Fourier transform of the interferogram.

Spectra measured with the Tsukuba TCCON FTS were analyzed by using the GFIT nonlinear least-squares spectral fitting algorithm, which is used for retrievals across all TCCON stations (Wunch et al., 2011a).

TCCON XCO_2 is defined as the ratio of the CO_2 column amount to the dry-air column amount. To calculate

Table 1. Characteristics of the Tsukuba TCCON FTS.

Instrument type	Bruker IFS 120 HR
Beam splitter	CaF_2
Aperture size	0.5 mm
Detector	InGaAs (5500–10 500 cm^{-1}), Si diode (9200–14 000 cm^{-1})
Spectral resolution	0.02 cm^{-1}
Single-scan observation time	70 s

the dry-air column amount, the GFIT algorithm uses the measured O_2 column amount divided by the known dry-air mole fraction of O_2 (0.2095). The O_2 and CO_2 columns are measured simultaneously using the 7751–8000 cm^{-1} (1250–1290 nm) and 6180–6260 and 6297–6382 cm^{-1} (1567–1588 and 1597–1618 nm) spectral bands, respectively. XCO_2 is then obtained as follows:

$$XCO_2 = 0.2095 \cdot (CO_2\,\text{column}/O_2\,\text{column}) \quad (1)$$

By using the CO_2 to O_2 ratio, systematic and correlated errors present in both retrieved columns are minimized.

The precision of the FTS measurement of XCO_2 is better than 0.2 % under clear sky conditions (Washenfelder et al., 2006; Ohyama et al., 2009; Messerschmidt et al., 2010; Wunch et al., 2011a). All TCCON XCO_2 data are corrected for airmass-dependent artifacts (Wunch et al., 2010). Aircraft profiles obtained over many of these sites are used to empirically scale the TCCON data according to the WMO standard reference scale. The scaling factor of TCCON XCO_2 is 1.011. The uncertainty of TCCON XCO_2 associated with the FTS measurement after scaling by 1.011 has been estimated to be 0.8 ppm (2σ) by comparing TCCON retrievals with many different aircraft-measured profiles (Wunch et al., 2010).

In 2010, Tsukuba TCCON FTS data were calibrated against data from three aircraft flights and tower measurements of CO_2 concentrations, and an additional bias of 1.32 ± 0.46 ppm (1σ) was added after airmass-dependent artifact correction and 1.011 scaling (Tanaka et al., 2012). This bias correction was reasonable (Wunch et al., 2011b). Here we use these bias-corrected Tsukuba TCCON XCO_2 data. About 0.3 ppm and 1 ppm is thought to be due to ghost (laser sampling error of FTS) and instrumental line shape (ILS) of Tsukuba TCCON FTS, respectively.

2.3 Comparison

We compared GOSAT SWIR XCO_2 data obtained over Tsukuba on 9 days between September 2009 and March 2010 with Tsukuba TCCON data, using the mean values measured at Tsukuba within 30 min of the GOSAT overpass time (around 12:54 LT) (Fig. 1; Table 2). The small number of comparison is due to severe co-location criterion. The distance from the center of the GOSAT field-of-view to the TCCON station was very small (less than 3 km) since we used the GOSAT data observed over Tsukuba TCCON site. The distance of lidar and Tsukuba TCCON site is 513 m. The severe co-location criterion is to exclude the spatial difference of aerosols and cirrus clouds of which variations are comparatively large.

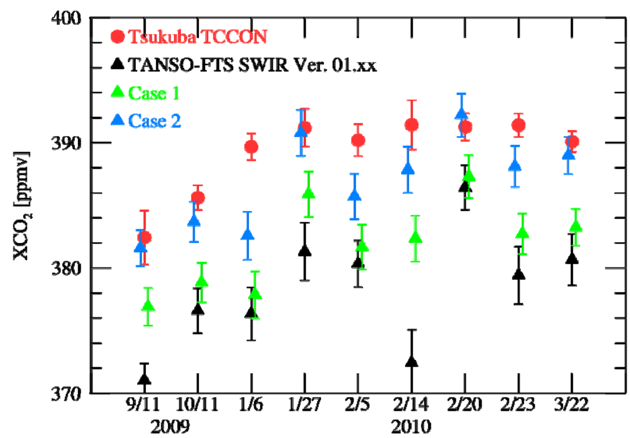

Fig. 1. Comparison of TANSO-FTS SWIR XCO_2 (Ver. 01.xx) data with the Tsukuba TCCON, Case 1 and Case 2 XCO_2 results. The Case 1 and Case 2 XCO_2 are retrieved using Kurucz's and Toon's solar irradiance data, respectively. Both cases are taking into account the vertical profiles of two types of aerosols and cirrus clouds determined from lidar and sky radiometer (Table 5). The error bars for the Tsukuba TCCON data and the retrieved XCO_2 are also shown.

The GOSAT SWIR XCO_2 data obtained on 14 February 2010 did not converge within the pre-determined maximum iteration number of 20, so we used the XCO_2 value obtained at the 20th iteration. The average difference between GOSAT SWIR XCO_2 and Tsukuba TCCON XCO_2 was -10.99 ± 3.83 ppm, based on all data summarized in Table 2. This is larger than the value of -7.70 ± 2.75 ppm at Tsukuba for an extended comparison and excluding data not meeting quality control criteria (Morino et al., 2011). Next we investigate these results by comparing them with lidar data obtained simultaneously with the GOSAT and Tsukuba TCCON FTS data.

Table 2. Comparison of GOSAT SWIR XCO_2 (A) with Tsukuba TCCON XCO_2 (B) and the quality control items not satisfactory for data release. Aerosol optical thickness (AOT) was retrieved at the wavelength of 1600 nm. SNR is signal-to-noise ratio.

Date	A (ppm)	B (ppm)	A–B (ppm)	AOT	Quality control items
11 Sep 2009	371.02	382.44	−11.42	1.092	AOT > 0.5
11 Oct 2009	376.58	385.62	−9.04	0.429	
6 Jan 2010	376.34	389.68	−13.34	0.233	SNR = 94.5 at Band 1
27 Jan 2010	381.31	391.20	−9.89	0.410	
5 Feb 2010	380.33	390.20	−9.87	0.141	
14 Feb 2010	372.42	391.43	−19.01	0.928	not converged, AOT > 0.5
20 Feb 2010	386.41	391.27	−4.86	0.176	
23 Feb 2010	379.41	391.41	−12.00	0.453	
22 Mar 2010	380.66	390.10	−9.44	1.011	AOT > 0.5

Table 3. Characteristics of the two-wavelength polarization lidar.

Transmitter		
Laser	Nd:YAG	
Wavelength	532 nm	1064 nm
Pulse energy	150 mJ	150 mJ
Pulse repetition rate	10 Hz	
Beam divergence	0.2 mrad	
Receiver		
Telescope type	Ritchy-Chretien (advanced)	
Telescope diameter	30.5 cm	
Field of view (full angle)	1.0 mrad	
Interference filter (FWHM)	0.28 nm	0.38 nm
Transmission	58 %	58 %
Polarization measurement	Yes	No
Number of receiving channel	3 (P:2, S:1)	1
Detector	PMT (R3234-01)	APD (Silicon)
Transient recorder	12bit A/D + PC	12 bit A/D
Minimum time resolution	1 min	
Minimum altitude resolution	7.5 m	

3 Lidar observations of aerosols and thin cirrus clouds over Tsukuba and the influence of high-altitude particles on GOSAT SWIR XCO_2

A compact lidar, based on a Nd:YAG laser, was developed to observe vertical distributions of thin cirrus clouds and aerosols and evaluate the influence of these particles on GOSAT SWIR XCO_2 data. Two laser wavelengths of 1064 nm ($\lambda1$) and 532 nm ($\lambda2$) are transmitted into the atmosphere through a beam expander. The backscattered light from the upper atmosphere is collected by a telescope and then divided into $\lambda1$ and $\lambda2$ by a dichroic mirror, and $\lambda2$ is further divided into a parallel (P) and a perpendicular component (S) by a polarizer. $\lambda1$ is detected by an avalanche photodiode (APD) and $\lambda2$ by photomultiplier tubes (PMTs). The output signals are processed by transient recorders with an analog/digital converter (A/D) and a photon counter (PC). Table 3 summarizes the characteristics of the lidar (Uchino et al., 2010).

The backscattering ratio R is defined as

$$R = (BR + BA)/BR \tag{2}$$

where BR and BA are the Rayleigh and Mie backscattering coefficients, respectively. Backscattering ratio profiles are derived by the inversion method (Fernald, 1984). We assumed the lidar ratio (extinction to backscatter ratio) to be 50 sr for aerosols (Sakai et al., 2003; Cattrall et al., 2005) and 20 sr for cirrus clouds (Sakai et al., 2003). To calculate BR, we used the atmospheric molecular density profiles obtained by operational radiosondes at the Aerological Observatory of the Japan Meteorological Agency (JMA) (36.06° N, 140.13° E) in Tsukuba.

The total depolarization ratio (Dep) is defined as

$$\mathrm{Dep} = S/(P+S)\cdot 100(\%) \tag{3}$$

where P and S are the parallel and perpendicular components of the backscattered signals. Dep indicates whether the particles are spherical or non-spherical, with large values indicating non-spherical particles. The wavelength exponent, Alp, which shows whether the Mie particles are small or large, is defined by

$$BA(\lambda) \propto \lambda^{-\mathrm{Alp}} \tag{4}$$

Larger values of Alp indicate smaller particles.

Figure 2 shows vertical profiles of R, Dep, and Alp observed on 14, 20, and 23 February 2010. The lidar observations were made during a period of about 10 min as GOSAT passed over Tsukuba. The vertical resolution used for the analysis was 150 m. On 14 February 2010, there were thin cirrus clouds at altitudes of 6.1–10.9 km and aerosols below 3 km. The partial optical thickness at altitudes of 0.4–30 km, Tau (0.4–30 km), was 0.24 at 532 nm (Fig. 2). The optical thickness from the surface to the top of the atmosphere could not be obtained below 0.4 km because the beam overlap between the lidar transmitter and receiver was not perfect. Lidar measurements of stratospheric aerosols above 15 km were observed at night (Uchino et al., 2010). In contrast to 14 February, 20 February 2010 was a comparatively clear day with aerosols in the boundary layer, and Tau (0.4–30 km) was estimated to be 0.1. On 23 February, the high-altitude aerosols observed at altitudes of 1–5 km were likely dust particles, because Dep was large, indicating non-spherical particles. Tau (0.4–30 km) was 0.16.

The difference between GOSAT SWIR XCO_2 and Tsukuba TCCON XCO_2 values was the largest (-19.01 ppm) on 14 February 2010 (Table 2). The difference was small (-4.86 ppm) on 20 February, and it was somewhat large (-12.00 ppm) on 23 February. The cirrus clouds on 14 February 2010 might have influenced the GOSAT retrieval. There were also thin cirrus clouds around 10.9–11.2 km altitude on 11 September 2009, when the difference was also relatively large (-11.42 ppm). Our results indicate that the retrieval of GOSAT SWIR XCO_2 data is greatly influenced by high-altitude aerosols and thin cirrus clouds and their optical thickness.

The current version of the retrieval algorithm (Ver. 01.xx) assumes that atmospheric aerosols are uniformly distributed from the ground surface to 2 km altitude. Next we show that GOSAT SWIR XCO_2 data were improved when the vertical distribution of the optical thicknesses of aerosols and the thin cirrus clouds observed by lidar and sky radiometer were taken into account.

4 Improvement of GOSAT SWIR XCO_2 retrieval

4.1 Vertical profiles of aerosol species and cirrus clouds

Vertical profiles and optical properties of aerosols and cirrus clouds used in the retrieval analysis were prepared based on the lidar and sky radiometer measurements. The sky radiometer can measure aerosol optical thickness and single scattering albedo at four wavelengths (400, 500, 675, and 870 nm), and the Angstrom exponent can be estimated from the optical thickness at these four wavelengths (Shiobara et al., 1991; Kobayashi et al., 2006). A large value of the Angstrom exponent indicates small particles. Table 4 summarizes the aerosol optical thickness at 500 nm (τ_{500}), the single scattering albedo at 500 nm (ω_{500}), and the Angstrom exponent (α) at the GOSAT overpass times; the optical thickness at 532 nm (τ_{532}), calculated from the lidar measurement by extrapolating the value of BA at 0.4 km down to the ground surface, is also shown. The optical thickness of cirrus clouds is not included in τ_{532}, and it is approximately the same as τ_{500}. The Angstrom exponent of aerosols over Tsukuba was large except on 14 February, 23 February, and 22 March 2010 (Table 4). In addition, the values of ω_{500} were close to unity, indicating that the aerosol particles were small and non-absorbing (Table 4). The relatively small value of α on 14 February 2010 might reflect contamination by cirrus clouds, because the Dep value of the lidar measurement does not indicate the presence of large, non-spherical aerosol particles. We therefore assumed that, except on 23 February and 22 March 2010, the aerosols over Tsukuba were sulfate because the particles were small and non-absorbing.

Table 4. Optical thickness at 500 nm (τ_{500}), single-scattering albedo at 500 nm (ω_{500}), and Angstrom exponent (α) observed by sky radiometer, and aerosol optical thickness at 532 nm (τ_{532}) determined by lidar at Tsukuba.

Date	Sky radiometer			Lidar
(yyyy/mm/dd)	τ_{500}	ω_{500}	α	τ_{532}
2009/09/11	0.276	0.956	2.102	0.201
2009/10/11	0.087	0.840	2.095	0.098
2010/01/06	0.079	1.000	2.120	0.091
2010/01/27	no data	no data	no data	0.160
2010/02/05	0.093	1.000	2.364	0.146
2010/02/14	0.230	1.000	1.534	0.165
2010/02/20	0.109	0.999	2.130	0.116
2010/02/23	0.279	0.997	1.416	0.181
2010/03/22	0.180	0.999	0.785	0.187

On 23 February and 22 March, the vertical Dep profiles indicate the presence of large, non-spherical dust-like particles at 2–4 km altitude. We assumed small, non-absorbing aerosols to be sulfate and large particles to be dust. We calculated the optical properties of sulfate aerosols following Takemura et al. (2002), but using a reduced width in the size distribution as suggested by Schutgens et al. (2010). For the dust aerosol model, we used the mineral-transported component of the model of Hess et al. (1998). Using these aerosol models, we determined the dry-mass fraction of sulfate such that the Angstrom exponent of the sulfate-dust

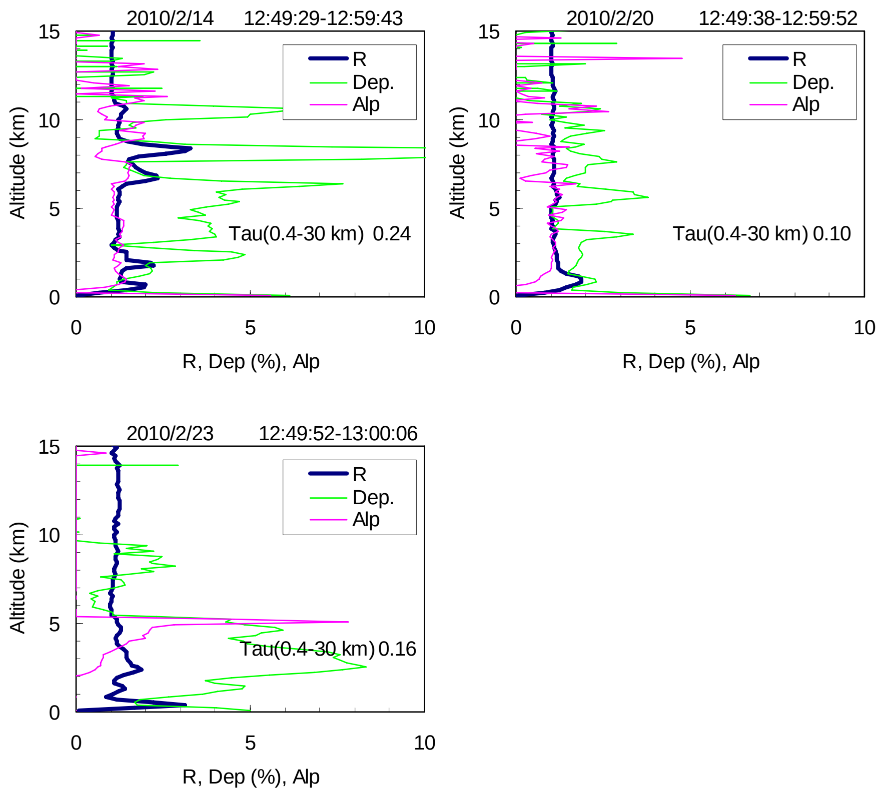

Fig. 2. Vertical profiles of the backscattering ratio R, total depolarization ratio Dep, and wavelength exponent Alp, observed by lidar on 14, 20, and 23 February 2010. Tau (0.4–30 km) is the partial optical thickness at altitudes of 0.4–30 km at 532 nm.

Table 5. Physical parameters currently used for retrieval (Ver. 01.xx) and three case studies showing decreased biases of GOSAT SWIR XCO_2 data.

	Aerosol vertical profile	Aerosol optical characteristics	Cirrus	Solar irradiance database
Ver. 01.xx	0∼2 km	SPRINTARS	No	Kurucz
Case 1	lidar	sulfate and dust	Yes	Kurucz
Case 2	lidar	sulfate and dust	Yes	Toon
Case 3	Retrieved (SPRINTARS as a priori data)	SPRINTARS	Yes	Toon

mixture agreed with that derived from the sky radiometer observations.

The vertical profiles of the extinction coefficient and the optical thicknesses of sulfate particles and cirrus clouds on 14 February 2010 are shown in Fig. 3, and those of sulfate and dust particles on 23 February 2010 are shown in Fig. 4. Similarly, we obtained vertical profiles of aerosols and cirrus clouds for the other days by using lidar and sky radiometer data observed at Tsukuba.

4.2 Case 1 XCO_2 retrieved using the vertical profiles of particles observed by lidar and sky radiometer

We retrieved XCO_2 (Case 1 XCO_2) by taking account of the vertical profiles of the two types of aerosols and cirrus clouds determined from lidar and sky radiometer data (Table 5, Case 1). In Case 1, we modified the operational Ver. 01.xx algorithm as follows. The uniform aerosol distribution up to 2 km altitude was replaced by the vertical profile derived from lidar measurements, as shown in Figs. 3 and 4. The aerosol optical thickness was then retrieved by scaling

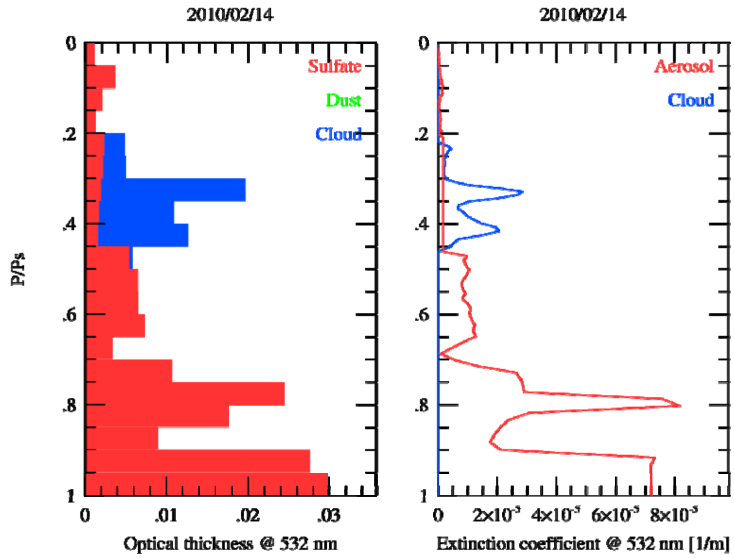

Fig. 3. Vertical profiles of the optical thicknesses (left panel) and extinction coefficients (right panel) of sulfate and cirrus cloud particles at 532 nm on 14 February 2010. The vertical scale is pressure normalized to surface pressure. The values of 0.5 and 0.1 correspond to altitudes of about 5.5 and 16 km, respectively.

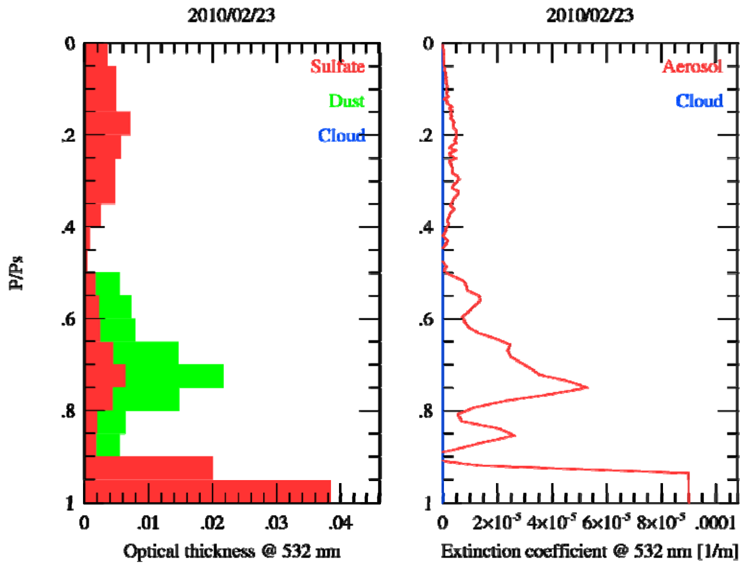

Fig. 4. Vertical profiles of optical thicknesses (left panel) and extinction coefficients (right panel) of sulfate and dust particles at 532 nm on 23 February 2010.

the vertical profile. Then we used Mie theory to derive the aerosol optical properties by assuming a mixture of sulfate and dust; for the operational algorithm we adopted aerosol optical properties estimated by the aerosol transport model SPRINTARS (Ver. 3.54) (Takemura et al., 2000). In addition, cirrus clouds were included in the forward model on 11 September 2009 and 14 February 2010, when lidar measurements showed that they were present. The optical thickness of the cirrus clouds was retrieved by scaling the vertical profile observed by lidar. To estimate the optical properties of ice crystals in the cirrus clouds, we adopted the Cirrus 3 model of Hess et al. (1998).

We plotted these retrieved values as the Case 1 XCO_2 against the Tsukuba TCCON values (Fig. 1). The difference between the Case 1 XCO_2 and the Tsukuba TCCON XCO_2 data was -7.40 ppm $\pm$ 2.39 ppm; thus, these Case 1 XCO_2

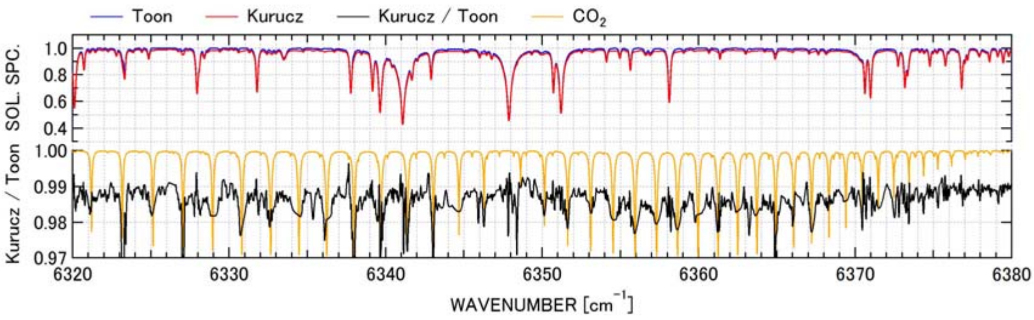

Fig. 5. The Kurucz's and Toon's solar spectrum and the ratio are plotted with CO_2 absorption lines.

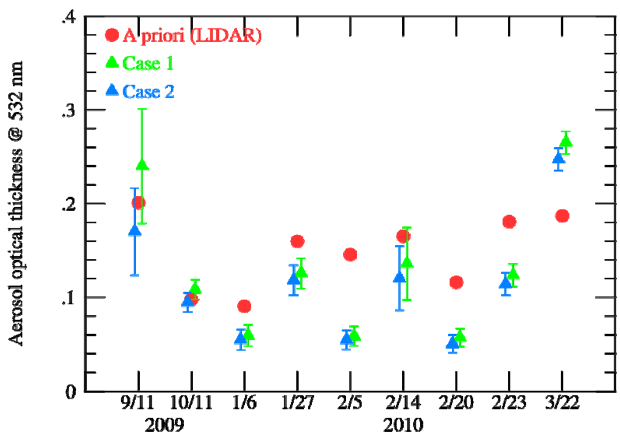

Fig. 6. Comparison of retrieved optical thickness at 532 nm (Case 1 and Case 2) with a priori values estimated from lidar measurements. The error bars of the retrieved values are also shown.

data are closer to the TCCON data than the SWIR Ver. 01.xx results shown in Fig. 1. In particular, the data for 11 September 2009 and 14 February 2010, when aerosol optical thickness was large (Table 4) and cirrus clouds were present, and on 23 February and 22 March 2010, when aerosol optical thickness was large, were greatly improved. Nevertheless, although the negative bias in XCO_2 was reduced to two thirds that obtained with the operational algorithm, it was not eliminated. For the models of Cirrus 1, 2 and 3 by Hess et al. (1998), the differences of the retrieved XCO_2, surface pressure, and AOT were 0.3 ppm, 0.5 hPa, and 0.01 respectively, and the above-mentioned result was rather stable. However, it is better to obtain more examples of thin cirrus clouds before reaching a general conclusion.

4.3 Solar irradiance database

Although a high-resolution solar irradiance database is needed to simulate a TANSO-FTS measured spectrum, few such solar irradiance databases are available. The GOSAT SWIR retrieval analysis used the high-resolution solar irradiance database (0.004 to 0.01 cm^{-1}) of R. Kurucz (http://kurucz.harvard.edu/sun/irradiance2008/). This database was created from spectra measured with a ground-based high-resolution FTS at Kitt Peak National Observatory (Arizona, USA) by removing the absorption structure due to the earth's atmosphere. However, as shown in Fig. 5, we noticed a CO_2 absorption structure in the spectral residual between the measured spectrum and the spectrum simulated by the forward spectral model, whereas when we used a solar spectrum database provided by G. C. Toon (personal communication, 2011; Toon et al., 1999), we confirmed no CO_2 absorption structure in the spectral residuals. We thus decided to use Toon's solar irradiance database. We also applied the low-frequency baseline correction in the current Ver. 01.xx retrieval to Toon's solar irradiance database. The low-frequency baseline correction is to fit the baseline of the solar irradiance spectra to calibration data of the solar irradiance by a diffuser installed on the TANSO-FTS.

4.4 Case 2

We retrieved XCO_2 (Case 2 XCO_2) data by using Toon's solar irradiance data instead of Kurucz's data and by taking into account the vertical profiles of the two types of aerosols and cirrus clouds determined by lidar and sky radiometer (Table 5, Case 2), and plotted these Case 2 XCO_2 values against the Tsukuba TCCON data (Fig. 1). The difference between the Case 2 XCO_2 and Tsukuba TCCON XCO_2 data was -2.43 ± 2.45 ppm. Thus, the Case 2 XCO_2 data were much closer to the Tsukuba TCCON XCO_2 data than the GOSAT SWIR (Ver. 01.xx) data (Fig. 1). A lidar point measurement is not always representative for a GOSAT pixel with 10 km in diameter when aerosols and thin cirrus clouds vary rapidly in space and time. This is one of the reasons of remaining discrepancies in Case 2. For example, thin cirrus clouds were variable in time on 14 February.

We compared the retrieved optical thickness at 532 nm with that of the a priori lidar data (Fig. 6) and found that, in general, the retrieved aerosol optical thickness was similar to the a priori value. There is no large difference of

AOT for Case 1 and Case 2. In spite of longer wavelength, AOT of Ver. 01.xx in Table 2 is larger than that in Case 1 and Case 2. We also compared the a priori surface pressure, obtained by interpolating in both time and space the Objective Analysis Data (the gridded meteorological data analyzed from the global observational data) of JMA to obtain values for Tsukuba, with the retrieved values (Fig. 7). The difference between the a priori and the Case 2 retrieved surface pressure was small except on 11 October 2009 compared with that for the Case 1. Therefore, it is reasonable to infer that the Case 2 XCO_2 data are reliable. However, the retrieved surface pressures improved largely compared with those of Ver. 01.xx. The vertical distributions of aerosol and cirrus clouds contribute to a large change in surface pressure, and the aerosol type next with moderate change. If we take into account of the aerosol vertical distribution, the spectral residual (chi-squared) improved in Band 1. There is no large difference of the spectral residuals in Band 1 and Band 2 between Case 1and Case 2.

Apart from modeling of aerosols and solar irradiance database, the forward model of the present analysis is the same as that of Ver. 01.xx algorithm described in Yoshida et al. (2011). Line mixing and collision-induced absorption are included in the calculation of O_2 A Band absorption. Fluorescence is not included in the forward model. Retrievals of surface pressure and aerosols can also be affected by a zero-level offset, which is observed in Band 1 spectra and is thought to be caused by the instrument's non-linearity (Butz et al., 2011). To address this issue, we made additional calculations in which a zero-level offset was simultaneously retrieved. We found that there is little effect of a zero-level offset for 6 data from 6 January to 23 February since the signal levels were sufficiently low. For 6 data, the retrieved surface pressures are higher ($\sim$5 hPa) than the a priori values, and it could be due to the spectroscopic line parameter database in the O_2 A band.

4.5 Improved 3-band retrieval (Case 3)

In this study, we demonstrated that the negative bias of 10.99 ± 3.83 ppm for all GOSAT SWIR XCO_2 data in Table 2 at the Tsukuba TCCON site could be reduced to 7.40 ± 2.39 ppm by taking into account the vertical profiles of aerosols and cirrus clouds observed by lidar and sky radiometer. The negative bias in XCO_2 was then further reduced to 2.43 ± 2.45 ppm by using Toon's solar irradiance data instead of Kurucz's data.

These results show that vertical profiles of aerosol species and cirrus clouds must be considered in the retrieval algorithm in order to improve the data quality of the global GOSAT SWIR XCO_2 when lidar observations are not available. One of the simplest ways to improve the treatment of aerosols would be to incorporate vertical profiles of aerosols obtained from SPRINTARS in the forward model. Aerosol vertical profiles simulated by SPRINTARS, however, are not

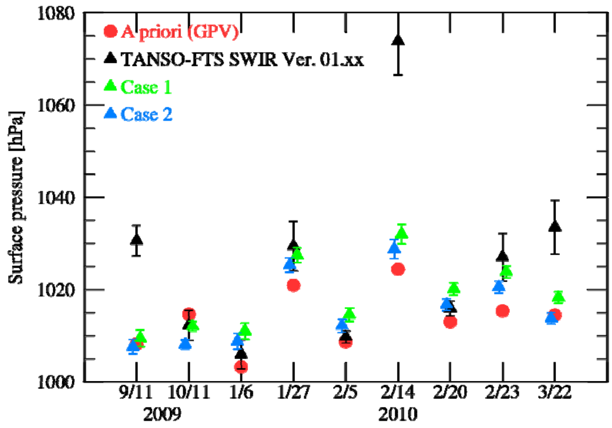

Fig. 7. Comparison of retrieved surface pressure (Case 1 and Case 2) with a priori pressure. The error bars of the retrieved values are also shown.

sufficient, as shown by comparing the SPRINTARS aerosol profile with that observed by lidar (Fig. 8). Therefore, as the first step, we simultaneously retrieved XCO_2 (Case 3 XCO_2; Table 5, Case 3) and the vertical profile of aerosol optical thickness based on the a priori aerosol optical thickness profile calculated by SPRINTARS. In Case 3, the optical thickness and cloud-top pressure of the cirrus clouds were also retrieved simultaneously. The cloud-bottom pressure was modeled as a linear function of the cloud-top pressure, as suggested by N. Eguchi (personal communication, 2011; Eguchi et al., 2007), and the cirrus clouds were assumed to be distributed uniformly in the vertical direction. In addition, Band 3 spectra (4790–4910 cm^{-1}) were also utilized in Case 3 for higher retrieval accuracy of the vertical aerosol profiles.

The Case 3 and Tsukuba TCCON XCO_2 values are shown in Fig. 9. We also plot the a priori XCO_2values calculated by the National Institute for Environmental Studies Transport Model (NIES TM) and their errors which were assumed to be the 100 times of the original CO_2 variance-covariance matrix (refer to Yoshida et al., 2011). The difference between the Case 3 XCO_2 and the Tsukuba TCCON XCO_2 data was 0.17 ± 1.49 ppm. The standard deviation of 1.49 ppm ($1\ \sigma$) is larger than about 1 ppm which is estimated theoretically optimal retrieval precision due to SNR over most land surfaces for SZAs less than 70 degrees (Boesch et al., 2011). As the errors of the a priori values are $\sim$16 ppm, the retrieved XCO_2 could not be over-constrained by the a priori. Although information on the vertical profiles of aerosols and cirrus clouds observed by lidar was not used in retrieving the Case 3 XCO_2, the Case 3 values were considerably closer to the Tsukuba TCCON XCO_2 values than current retrievals by GOSAT SWIR XCO_2 (Fig. 1). We also found that use of Band 3 increased XCO_2 by about 2 ppm, but we have not yet identified the origin of this difference. It might be attributed

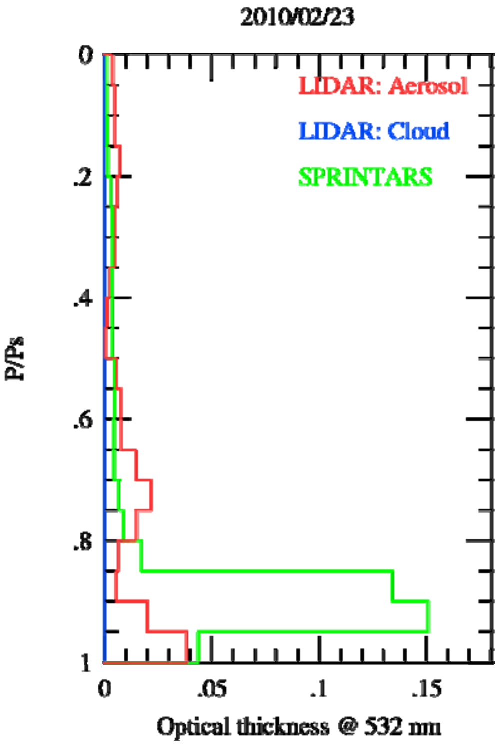

Fig. 8. Vertical profiles of aerosol optical thickness measured by lidar and simulated by SPRINTARS at 532 nm on 23 February 2010.

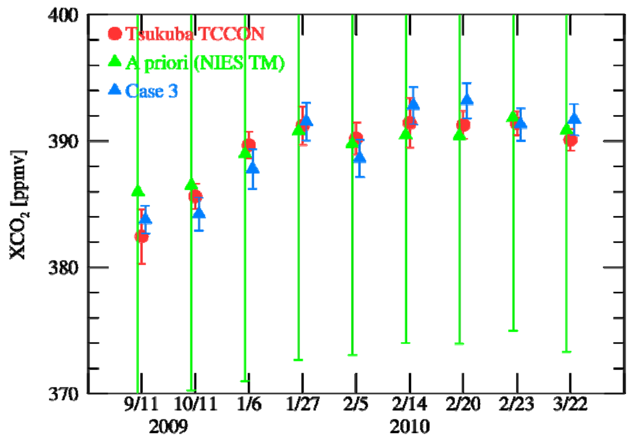

Fig. 9. Comparison of Case 3 XCO_2 data, obtained by retrieving the aerosol profile based on the a priori vertical profile and fixed aerosol optical characteristics given by the SPRINTARS model, with the Tsukuba TCCON XCO_2 data (Table 5, Case 3). The used a priori values and their error bars are also shown.

to be spectroscopy. Both collisional narrowing and speed dependence of collisional broadening and shifting play a significant role near 1600 nm over a pressure range of 330–67 hPa (Long et al., 2011), where we do not take into account those effects.

Aerosol optical properties derived from SPRINTARS were used in both Case 3 and the current operational algorithm. The Case 3 XCO_2 results shown in Fig. 9 are promising. We know this study is only based on the performance for one site and we would need to carry out validation for other sites. An improved SPRINTARS might further improve the results. Therefore, it would be better to use a new SPRINTARS model in which AERONET observations are assimilated (Schutgens et al., 2010). Furthermore, SPRINTARS is being further improved by assimilation of lidar network and CALIOP data (Shimizu et al., 2004; Winker et al., 2007; Sekiyama et al., 2010).

5 Concluding remarks

Version 01.xx GOSAT SWIR XCO_2 data, released in August 2010, were compared with Tsukuba TCCON data. Comparison of lidar and sky radiometer observations with the GOSAT SWIR XCO_2 data clearly showed that high-altitude aerosols and thin cirrus clouds had a large impact on GOSAT SWIR XCO_2. The current retrieval algorithm (Ver. 01.xx) for XCO_2 and XCH_4 from the GOSAT TANSO-FTS SWIR observation data assumes that atmospheric aerosols are uniformly distributed from the ground surface to 2 km altitude. By taking into account the actual vertical distributions of aerosols determined by lidar and sky radiometer over Tsukuba, and by using Toon's solar irradiance database instead of Kurucz's database, the difference between GOSAT SWIR XCO_2 data and the Tsukuba TCCON XCO_2 found in the Ver. 01.xx results was reduced. The 3-band retrieval approach where the aerosol and cirrus profiles were retrieved gave us the best results and the retrieved XCO_2 data followed the seasonal cycle of ∼8 ppm observed at Tsukuba TCCON site of which value was consistent to the result by Ohyama et al. (2009).

In this paper we concentrated our attention on resolving the large bias of the Ver. 01.xx results shown by Morino et al. (2011). However, it is important to reduce the regional biases due to distinct regional patterns of aerosols and cirrus clouds for application of inverse modeling. The 3-band retrieval method where the aerosol and cirrus profiles are retrieved has a possibility of reducing the standard deviations of the biases and the regional biases. Recently the NASA Atmospheric CO_2 Observations from Space (ACOS) team applied this 3-band retrieval to GOSAT data (O'Dell et al., 2012; Crisp et al., 2012). In the near future, we plan to incorporate the vertical distributions of aerosols at altitudes above 2 km in the GOSAT SWIR retrieval algorithm.

Acknowledgements. We are grateful to G. C. Toon for making his solar irradiance data available to us. We also acknowledge N. Eguchi for valuable information on cirrus clouds. The authors wish to thank three anonymous referees for their helpful and insightful comments. The Meteorological data were supplied by the Japan Meteorological Agency. This research was supported in part by the Environment Research and Technology Development Fund (A-1102) of the Ministry of the Environment, Japan.

Edited by: M. K. Dubey

References

Boesch, H., Baker, D., Connor, B., Crisp, D., and Miller, C.: Global characterization of CO_2 column retrievals from shortwave-infrared satellite observations of the Orbiting Carbon Observatory-2 Mission, Remote Sens., 3, 270–304, doi:10.3390/rs3020270, 2011.

Butz, A., Hasekamp, O. P., Frankenberg, C., and Aben, I.: Retrievals of atmospheric CO_2 from simulated space-borne measurements of backscattered near-infrared sunlight: accounting for aerosol effects, Appl. Optics, 48, 3322–3336, 2009.

Butz, A., Guerlet, S., Hasekamp, O., Schepers, D., Galli, A., Aben, I., Frankenberg, C., Hartmann, J. -M., Tran, H., Kuze, A., Keppel-Aleks, G., Toon, G., Wunch, D., Wennberg, P., Deutscher, N., Griffith, D., Macatangay, R., Messerschmidt, J., Notholt, J., and Warneke, T.: Toward accurate CO_2 and CH_4 observations from GOSAT, Geophys. Res. Lett., 38, L14812, doi:10.1029/2011GL047888, 2011.

Cattrall, C., Reagan, J., Thome, K., and Dubovik, O.: Variability of aerosol and spectral lidar and backscatter and extinction ratios of key aerosol types derived from selected Aerosol Robotic Network locatios, J. Geophys. Res., 110, D10S11, doi:10.1029/2004JD005124, 2005.

Chevallier, F., Maksyutov, S., Bousquet, P., Bréon, F.-M., Saito, R., Yoshida, Y., and Yokota, T.: On the accuracy of the CO_2 surface fluxes to be estimated from the GOSAT observations, Geophys. Res. Lett., 36, L19807, doi:10.1029/2009GL040108, 2009.

Connor, B., Boesch, H., Toon, G., Sen, B., Miller, C., and Crisp, D.: Orbiting Carbon Observatory: Inverse method and prospective error analysis, J. Geophys. Res., 113, D05305, doi:10.1029/2006JD008336, 2008.

Cox, P. M., Betts, R. A., Jones, C. D., Spall, S. A., and Totterdell, I. J.: Acceleration of global warming due to carbon-cycle feedbacks in a coupled climate model, Nature, 408, 184–187, 2000.

Crisp, D., Fisher, B. M., O'Dell, C., Frankenberg, C., Basilio, R., Bsch, H., Brown, L. R., Castano, R., Connor, B., Deutscher, N. M., Eldering, A., Griffith, D., Gunson, M., Kuze, A., Mandrake, L., McDuffie, J., Messerschmidt, J., Miller, C. E., Morino, I., Natraj, V., Notholt, J., O'Brien, D. M., Oyafuso, F., Polonsky, I., Robinson, J., Salawitch, R., Sherlock, V., Smyth, M., Suto, H., Taylor, T. E., Thompson, D. R., Wennberg, P. O., Wunch, D., and Yung, Y. L.: The ACOS CO_2 retrieval algorithm – Part II: Global X_{CO_2} data characterization, Atmos. Meas. Tech., 5, 687–707, doi:10.5194/amt-5-687-2012, 2012.

Eguchi, N., Yokota, T., and Inoue, G.: Characteristics of cirrus clouds from ICESat/GLAS observations, Geophys. Res. Lett., 34, L09810, doi:10.1029/2007GL029529, 2007.

Fernald, F. G.: Analysis of atmospheric lidar observations: some comments, Appl. Optics, 23, 652–653, 1984.

Hess, M., Koepke, P., and Schult, I.: Optical properties of aerosols and clouds: the software package OPAC, B. Am. Meteorol. Soc., 79, 831–844, 1998.

Houweling, S., Hartmann, W., Aben, I., Schrijver, H., Skidmore, J., Roelofs, G.-J., and Breon, F.-M.: Evidence of systematic errors in SCIAMACHY-observed CO_2 due to aerosols, Atmos. Chem. Phys., 5, 3003–3013, doi:10.5194/acp-5-3003-2005, 2005.

Hungershoefer, K., Bréon, F.-M., Peylin, P., Chevallier, F., Rayner, P., Klonecki, A., Houweling, S., and Marshall, J.: Evaluation of various observing systems for the global monitoring of CO_2 surface fluxes, Atmos. Chem. Phys., 10, 10503–10520, doi:10.5194/acp-10-10503-2010, 2010.

Intergovernmental Panel on Climate Change (IPCC), Climate change 2007: The Physical Science Basis: Contribution of Working Group I to the Fourth Assessment Report of the Intergovernmental Panel on Climate Change, edited by: Solomon, S., Qin, D., Manning, M., Chen, Z., Marquis, M., Averyt, K. B., Tignor, M., and Miller, H. L., Cambridge University Press, Cambridge, UK and New York, NY, USA, 996 pp. 2007.

Kobayashi, E., Uchiyama, A., Yamazaki, A., and Matsuse, K.: Application of the maximum likelihood method to the inversion algorithm for analyzing aerosol optical properties from sun and sky radiance measurements, J. Meteorol. Soc. Jpn., 84, 1047–1062, 2006.

Kuang, Z., Margolis, J., Toon, G., Crisp, D., and Yung, Y.: Spaceborne measurements of atmospheric CO_2 by high-resolution NIR spectrometry of reflected sunlight: An introductory study, Geophys. Res. Lett., 29, 1716, doi:10.1029/2001GL014298, 2002.

Kuze, A., Suto, H., Nakajima, M., and Hamazaki, T.: Thermal and near infrared sensor for carbon observation Fourier-transform spectrometer on the Greenhouse Gases Observing Satellite for greenhouse gases monitoring, Appl. Optics, 48, 6716–6733, 2009.

Long, D. A., Bielska, K., Lisak, D., Havey, D. K., Okumura, M., Miller, C. E., and Hodges, J. T.: The air-broadened, near-infrared CO_2 line shape in the spectrally isolated regime: Evidence of simultaneous Dicke narrowing and speed dependence, J. Chem. Phys., 135, 064308-1–064308-7, 2011.

Messerschmidt, J., Macatangay, R., Notholt, J., Petri, C., Warneke, T., and Weinzierl, C.: Side by side measurements of CO_2 by ground-based Fourier transform spectrometry (FTS), Tellus, 62B, 749–758, 2010.

Morino, I., Uchino, O., Inoue, M., Yoshida, Y., Yokota, T., Wennberg, P. O., Toon, G. C., Wunch, D., Roehl, C. M., Notholt, J., Warneke, T., Messerschmidt, J., Griffith, D. W. T., Deutscher, N. M., Sherlock, V., Connor, B., Robinson, J., Sussmann, R., and Rettinger, M.: Preliminary validation of column-averaged volume mixing ratios of carbon dioxide and methane retrieved from GOSAT short-wavelength infrared spectra, Atmos. Meas. Tech., 4, 1061–1076, doi:10.5194/amt-4-1061-2011, 2011.

O'Dell, C. W., Connor, B., Bösch, H., O'Brien, D., Frankenberg, C., Castano, R., Christi, M., Eldering, D., Fisher, B., Gunson, M., McDuffie, J., Miller, C. E., Natraj, V., Oyafuso, F., Polonsky, I., Smyth, M., Taylor, T., Toon, G. C., Wennberg, P. O., and Wunch, D.: The ACOS CO_2 retrieval algorithm – Part 1: Description and validation against synthetic observations, Atmos. Meas. Tech., 5, 99–121, doi:10.5194/amt-5-99-2012, 2012.

Ohyama, H., Morino, I., Nagahama, T., Machida, T., Suto, H., Oguma, H., Sawa, Y., Matsueda, H., Sugimoto, N., Nakane, H., and Nakagawa, K.: Column-averaged volume mixing ratio of CO_2 measured with ground-based Fourier transform spectrometer at Tsukuba, J. Geophys. Res., 114, D18303, doi:10.1029/2008JD011465, 2009.

Rayner, P. J. and O'Brien, D. M.: The utility of remotely sensed CO_2 concentration data in surface source inversions, Geophys. Res. Lett., 28, 175–178, 2001.

Reuter, M., Buchwitz, M., Schneising, O., Heymann, J., Bovensmann, H., and Burrows, J. P.: A method for improved SCIAMACHY CO_2 retrieval in the presence of optically thin clouds, Atmos. Meas. Tech., 3, 209–232, doi:10.5194/amt-3-209-2010, 2010.

Sakai, T., Nagai, T., Nakazato, M., Mano, Y., and Matsumura, T.: Ice clouds and Asian dust studied with lidar measurements of particle extinction-to-backscatter ratio, particle depolarization, and water-vapor mixing ratio over Tsukuba, Appl. Optics, 42, 7103–7116, 2003.

Schutgens, N. A. J., Miyoshi, T., Takemura, T., and Nakajima, T.: Applying an ensemble Kalman filter to the assimilation of AERONET observations in a global aerosol transport model, Atmos. Chem. Phys., 10, 2561–2576, doi:10.5194/acp-10-2561-2010, 2010.

Sekiyama, T. T., Tanaka, T. Y., Shimizu, A., and Miyoshi, T.: Data assimilation of CALIPSO aerosol observations, Atmos. Chem. Phys., 10, 39–49, doi:10.5194/acp-10-39-2010, 2010.

Shimizu, A., Sugimoto, N., Matsui, I., Arao, K., Uno, I., Murayama, T., Kagawa, N., Aoki, K., Uchiyama, A., and Yamazaki, A.: Continuous observations of Asian dust and other aerosols by polarization lidars in China and Japan during ACE-Asia, J. Geophys. Res., 109, D19S17, doi:10.1029/2002JD003253, 2004.

Shiobara, M., Hayasaka, T., Nakajima, T., and Tanaka, M.: Aerosol monitoring using a scanning spectral radiometer in Sendai, Japan, J. Meteorol. Soc. Jpn., 69, 57–70, 1991.

Takemura, T., Okamoto, H., Maruyama, Y., Numaguti, A., Higurashi, A., and Nakajima, T.: Global three-dimensional simulation of aerosol optical thickness distribution of various origins, J. Geophys. Res., 105, 17853–17873, 2000.

Takemura, T., Nakajima, T., Dubovik, O., Holben, B. N., and Kinne, S.: Single-scattering albedo and radiative forcing of various aerosol species with a global three-dimensional model, J. Climate, 15, 333–352, 2002.

Tanaka, T., Miyamoto, Y., Morino, I., Machida, T., Nagahama, T., Sawa, Y., Matsueda, H., Wunch, D., Kawakami, S., and Uchino, O.: Aircraft measurements of carbon dioxide and methane for the calibration of ground-based high-resolution Fourier Transform Spectrometers and a comparison to GOSAT data measured over Tsukuba and Moshiri, Atmos. Meas. Tech. Discuss., 5, 1843–1871, doi:10.5194/amtd-5-1843-2012, 2012.

Toon, G. C., Blavier, J.-F., Sen, B., Salawitch, R. J., Osterman, G. B., Notholt, J., Rex, M., McElroy, C. T., and Russell III, J. M.: Ground-based observations of Arctic O_3 loss during spring and summer 1997, J. Geophys. Res., 104, 26497–26510, 1999.

Uchino, O., Sakai, T., Nagai, T., Sakashita, T., Suzuki, K., Shibata, T., Morino, I., and Yokota, T.: Lidar observation of stratospheric aerosols increased from the 2009 Mount Sarychev volcanic eruption, J. Remote Sens. Soc. Japan, 30, 149–155, 2010 (in Japanese).

Washenfelder, R. A., Toon, G. C., Blavier, J.-F., Yang, Z., Allen, N. T., Wennberg, P. O., Vay, S. A., Matross, D. M., and Daube, B. C.: Carbon dioxide column abundances at the Wisconsin Tall Tower site, J. Geophys. Res., 111, D22305, doi:10.1029/2006JD007154, 2006.

Winker, D. M., Hunt, W. H., and McGill, M. J.: Initial performance assessment of CALIOP, Geophys. Res. Lett., 34, L19803, doi:10.1029/2007GL030135, 2007.

WMO: The state of greenhouse gases in the atmosphere based on global observations through 2009, WMO Greenhouse Gas Bulletin, No. 6, 2010.

Wunch, D., Toon, G. C., Wennberg, P. O., Wofsy, S. C., Stephens, B. B., Fisher, M. L., Uchino, O., Abshire, J. B., Bernath, P., Biraud, S. C., Blavier, J.-F. L., Boone, C., Bowman, K. P., Browell, E. V., Campos, T., Connor, B. J., Daube, B. C., Deutscher, N. M., Diao, M., Elkins, J. W., Gerbig, C., Gottlieb, E., Griffith, D. W. T., Hurst, D. F., Jimènez, R., Keppel-Aleks, G., Kort, E. A., Macatangay, R., Machida, T., Matsueda, H., Moore, F., Morino, I., Park, S., Robinson, J., Roehl, C. M., Sawa, Y., Sherlock, V., Sweeney, C., Tanaka, T., and Zondlo, M. A.: Calibration of the Total Carbon Column Observing Network using aircraft profile data, Atmos. Meas. Tech., 3, 1351–1362, doi:10.5194/amt-3-1351-2010, 2010.

Wunch, D., Toon, G. C., Blavier, J.-F. L., Washenfelder, R. A., Notholt, J., Connor, B. J., Griffith, D. W. T., Sherlock, V., and Wennberg, P. O.: The Total Carbon Column Observing Network (TCCON), Phil. Trans. R. Soc. A., 369, 2087–2112, doi:10.1098/rsta.2010.0240, 2011a.

Wunch, D., Wennberg, P. O., Toon, G. C., Connor, B. J., Fisher, B., Osterman, G. B., Frankenberg, C., Mandrake, L., O'Dell, C., Ahonen, P., Biraud, S. C., Castano, R., Cressie, N., Crisp, D., Deutscher, N. M., Eldering, A., Fisher, M. L., Griffith, D. W. T., Gunson, M., Heikkinen, P., Keppel-Aleks, G., Kyr, E., Lindenmaier, R., Macatangay, R., Mendonca, J., Messerschmidt, J., Miller, C. E., Morino, I., Notholt, J., Oyafuso, F. A., Rettinger, M., Robinson, J., Roehl, C. M., Salawitch, R. J., Sherlock, V., Strong, K., Sussmann, R., Tanaka, T., Thompson, D. R., Uchino, O., Warneke, T., and Wofsy, S. C.: A method for evaluating bias in global measurements of CO_2 total columns from space, Atmos. Chem. Phys., 11, 12317–12337, doi:10.5194/acp-11-12317-2011, 2011.

Yoshida, Y., Ota, Y., Eguchi, N., Kikuchi, N., Nobuta, K., Tran, H., Morino, I., and Yokota, T.: Retrieval algorithm for CO_2 and CH_4 column abundances from short-wavelength infrared spectra observations by the Greenhouse gases observing satellite, Atmos. Meas. Tech., 4, 717–734, doi:10.5194/amt-4-717-2011, 2011.